PRELIMINARY GEOPHYSICAL SURVEY TO DETECT SIGNIFICANT SHALLOW VOIDS NEAR TIMPSON, TEXAS

by

Jeffrey G. Paine and Edward W. Collins
John A. and Katherine G. Jackson School of Geosciences
Bureau of Economic Geology
The University of Texas at Austin
University Station, Box X
Austin, Texas 78713
jeff.paine@beg.utexas.edu
(512) 471-1260

Report prepared for

Railroad Commission of Texas

Under Contract No. UTAA8-066

February 2009

Introduction

Researchers at the Bureau of Economic Geology, The University of Texas at Austin, noninvasively measured the electrical conductivity and seismic properties of the shallow subsurface at the Dempsey residence near Timpson, Texas. This preliminary survey was completed to determine whether there is geophysical evidence of significant near-surface voids related to historical lignite mining activities. Voids are potentially detectable using several geophysical methods. Mass deficits might be detected using sensitive gravimeters; nonconductive air filling voids in more conductive strata might be detected using resistivity or electromagnetic induction (EM) methods; and air that fills voids might have a lower seismic velocity than the surrounding strata and could be detected with seismic methods. At Timpson, we chose EM in an attempt to identify possible significant voids that reach within about 6 m of the ground surface. We also acquired a test set of seismic data across a known void beneath a concrete pad at the residence to determine whether the void influenced the seismic data enough to be useful in detecting similar unknown voids at this or other similar sites. This report briefly summarizes the results of our investigations.

Methods

During the late 1970's and early 1980's, investigators began developing and using EM instruments to measure ground conductivity noninvasively to depths ranging from less than 1 to more than 50 m (McNeill, 1980a). The EM method is popular because it can be rapidly and noninvasively applied. EM methods have proven to be effective in locating surface anomalies in the electrical conductivity of the ground associated with limestone karst development (Paine and Collins, 2001, 2003).

On October 29, 2008, Bureau staff conducted an EM survey and seismic test at the Dempsey residence near Timpson, Texas. The purpose of the EM survey was to determine whether there is evidence for the presence of significant voids within the exploration depth range of the EM instrument. We used a Geonics EM31 ground conductivity meter to measure apparent electrical conductivity of the ground at 206 locations surrounding the residence (fig. 1).

The Geonics EM31 is a frequency-domain EM instrument that noninvasively measures ground conductivity by creating a continuously changing magnetic field around a transmitter coil (Frischknecht and others, 1991). As the primary magnetic field changes, it induces currents to flow in the ground that are proportional in strength to the electrical conductivity of the ground. These ground currents create a secondary magnetic field. A second receiver coil is used to compare the strength and phase of the primary and secondary fields to determine an apparent conductivity of the ground. Soil and rock have low natural conductivities (McNeill, 1980b) that range from a few to a few hundred milliSiemens per meter (mSm). The instrument measures the apparent conductivity of the ground to an exploration depth governed by the primary frequency, the strength of the signal, and the conductivity of the ground. Lower frequencies, stronger signals, and more resistive ground all increase the effective exploration depth of the EM instrument. The EM31 operates at a primary frequency of 9800 Hz and a coil separation of 3.7 m. Exploration depth can be changed by altering the coil orientation; the vertical dipole configuration explores about twice as deep (to about 6 m) as the horizontal dipole configuration (to about 3 m). The horizontal dipole orientation responds disproportionately strongly to the shallower third of its nominal exploration depth, whereas the vertical dipole orientation responds disproportionately strongly to the center third of its nominal exploration depth (Geonics, 1991). Deeper exploration can be achieved using instruments operating at lower frequencies and greater coil separation. In addition to apparent conductivity, the instrument also measures the inphase response of the ground, a measure of how much of a phase shift is caused by the ground. Because metallic objects cause a significant phase shift, inphase measurements can be used to detect buried metal.

We recorded eight EM measurements at each of the 206 locations that were acquired on a 2-m grid. These included shallow (horizontal dipole, or hd) and deep (vertical dipole, or vd) conductivity in two directions (north-south and east-west), and the shallow and deep in-phase EM component in the two directions. Processing included calculating key combinations of the measurements, including the difference between the two directional measurements for a given coil orientation (hd or vd), gridding individual and calculated parameters, and creating a site-grid GIS to manage and analyze the data.

The seismic test was conducted across a known void covered by a concrete pad. The approach was to generate seismic energy on one side of the void, detect its arrival on the other side of the void, and look for delays in arrival times that would indicate the presence and approximate position of the void. We set up a rack of 18 receivers (40 Hz geophones) along site grid column 14 between rows 10.75 and 15 east of the concrete pad at a receiver spacing of 0.5 m (total length of the receiver spread was 8.5 m). Seismic sources at 1-m spacing were located west of the concrete pad along site grid column 10 between rows 12 and 16 (table 1). Seismic energy was provided by a hammer striking an aluminum plate. Multiple hammer blows were stacked at each of the 9 locations to improve the signal-to-noise ratio in the seismic data, which were recorded on a 24-channel Geometrics SmartSeis seismograph. Data were recorded for 64 milliseconds at a sample interval of 0.031 milliseconds for each source location. Processing included converting seismic records, picking consistent first-arrival times for each source-receiver pair, and calculating average propagation velocities for each source-receiver pair. Images of average seismic velocities in the space between the source and receiver lines were generated by assuming straight-line travel paths between sources and receivers and collating average velocities for different source-receiver pairs that cross common cells in the parallelogram between the source and receiver lines. Using all the 180 source-receiver pairs (10 source locations and 18 receiver locations; with one duplicate shot location) and a 0.2-m cell width, the tomographic image of the space between the lines was constructed from 7020 data points.

Table 1. Locations of seismic source points and receiver endpoints relative to the site grid (adjacent rows and columns are 2-m apart) for the 10 seismic data files.

	Source		**Geophone 1**		**Geophone 18**	
File	**Column**	**Row**	**Column**	**Row**	**Column**	**Row**
1.dat	10.024	13	14	10.75	14	15
2.dat	10.073	12	14	10.75	14	15
3.dat	10.035	12.5	14	10.75	14	15
4.dat	10.024	13	14	10.75	14	15
5.dat	10	13.5	14	10.75	14	15
6.dat	10	14	14	10.75	14	15
7.dat	10	14.5	14	10.75	14	15
8.dat	10	15	14	10.75	14	15
9.dat	10	15.5	14	10.75	14	15
10.dat	10	16	14	10.75	14	15

EM Results

Apparent conductivity data were acquired over much of an area measuring about 44 m in an east-west (grid) direction and 32 m in a north-south (grid) direction around the Dempsey residence (fig. 1). In the shallower instrument orientation (horizontal dipole; exploration depth nominally 3 m), measurements made in the north-south and east-west directions range from 10 to 101 mS/m (figs. 1 and 2), values that are typical for dry to moist clayey soils. Both apparent conductivity maps show elevated values on the north side of the house, near the slab and walkway south of the house, and near the carport. These high values are most likely affected by surface or shallowly buried conductive metal. A composite map depicting the average of the north-south and east-west values (fig. 3) helps isolate the highly conductive areas north and south-southeast of the house. Lowest conductivities are found north-northeast and east of the house toward and within a topographic low. The average inphase response for the shallow-exploring coil orientation (fig. 4) shows the highest values north of the house, near a gas tank northeast of the house, an area east of the slab over the known void, and near the carport. Strong inphase response to nearby metal and the coincidence of the high inphase response values to elevated shallow conductivity areas further suggests the presence of surface or buried metal in these areas.

Apparent conductivities measured with the deeper-exploring, vertical-dipole orientation are generally higher than those for the shallower orientation, ranging from 24 to more than 341 mS/m and averaging 73 mS/m. Higher conductivities in this orientation are likely caused by increased soil moisture content with increasing exploration depth. Nominal exploration depth for this orientation is about 6 m, insufficient to reach the anticipated depths of past mining activity. Data collected in the north-south direction show areas of elevated conductivity near the house, east of the slab, and near the carport (fig. 5). Similar high-conductivity patterns are evident on maps of data acquired in the east-west direction (fig. 6). A composite map constructed from the average north-south and east-west values (fig. 7) indicates extensive low-conductivity areas north-northwest of the house and east of the house in a topographic low and elevated conductivity values near the home, concrete slab over the void, and carport. The map constructed from the average inphase response for the vertical dipole orientation (fig. 8) is similar to that

constructed from the horizontal dipole data (fig. 4), with strong responses near the gas tank, north of the home, near the carport, and east of the concrete slab. These areas clearly indicate the presence of significant surface (gas tank, air conditioner, and carport) and buried metal (the area east of the slab). Smaller areas with less strong inphase response indicate the presence of smaller pieces of metal.

Neither the shallow- nor the deeper-exploring EM data strongly suggest the presence of significant voids within the exploration depth range of the instrument. Significant buried metal, particularly east of the slab, may indicate where prior collapse areas have been filled with material that includes metallic objects. Deeper-exploring instruments would be required to examine evidence for low-conductivity areas that might indicate the presence of voids at depths approaching 15 to 20 m, the anticipated depth of mine workings in this area.

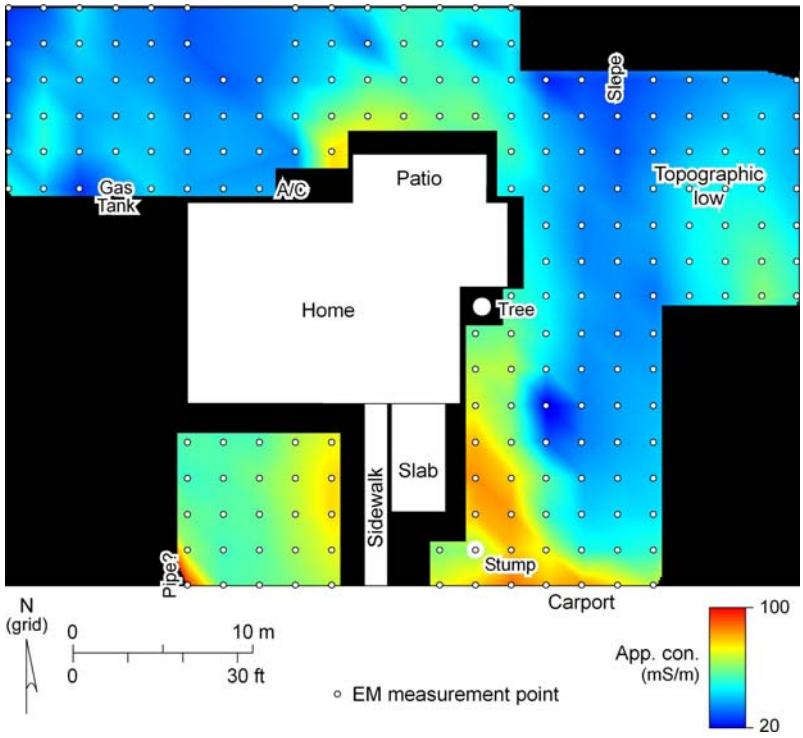

Figure 1. Apparent conductivity measured with a Geonics EM31 with the shallower-exploring horizontal-dipole orientation and north-south direction.

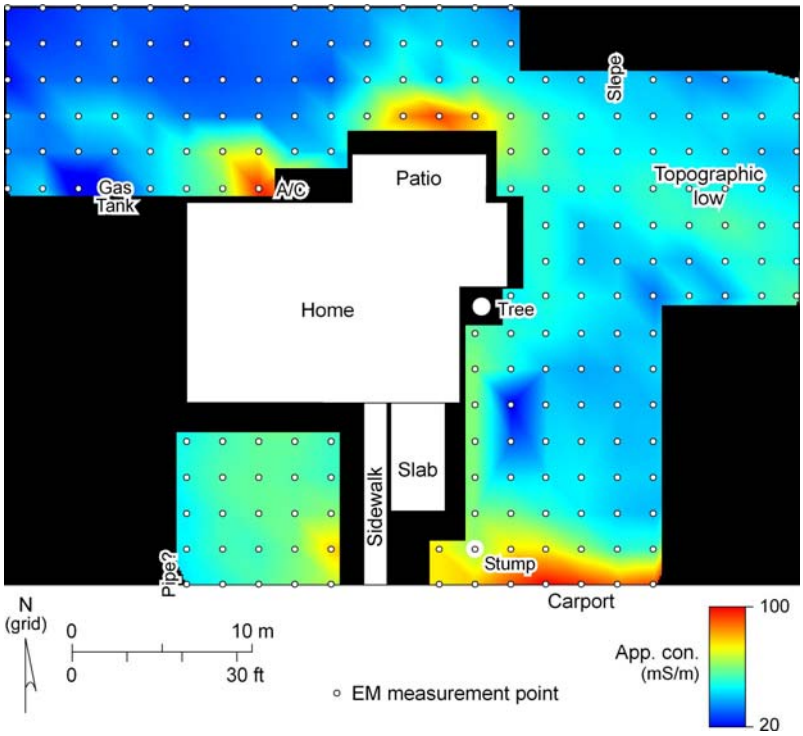

Figure 2. Apparent conductivity measured with a Geonics EM31 with the shallower-exploring horizontal-dipole orientation and east-west direction.

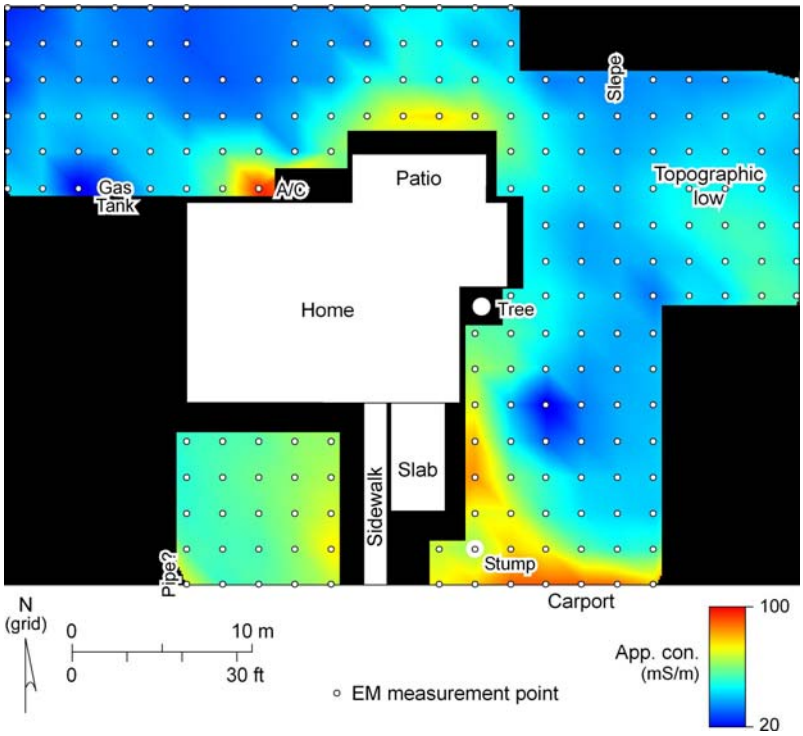

Figure 3. Average apparent conductivity measured with a Geonics EM31 with the shallow-exploring, horizontal-dipole orientation in both directions.

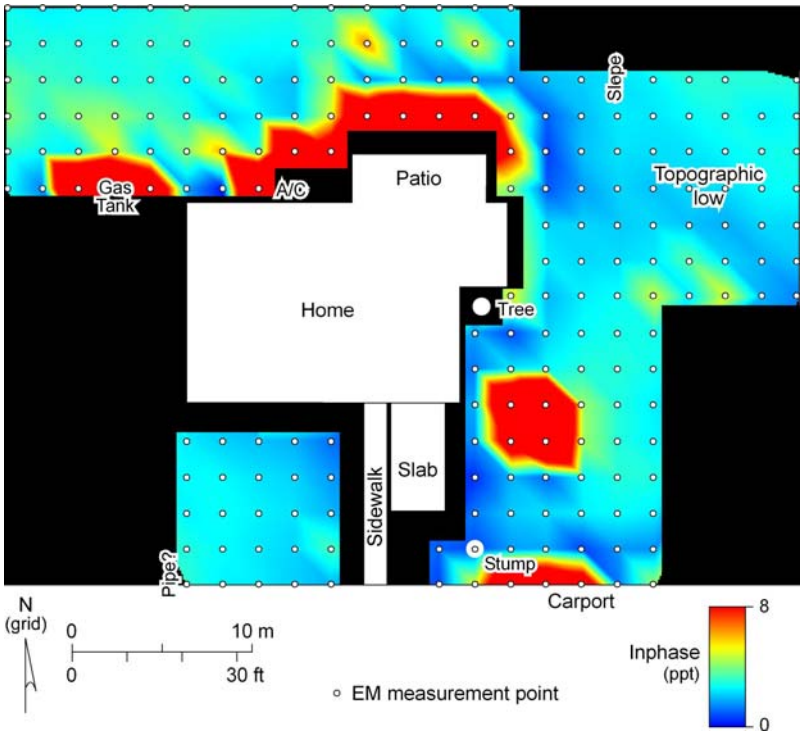

Figure 4. Average inphase response measured with a Geonics EM31 with the shallower-exploring horizontal-dipole orientation in the north-south and east-west directions.

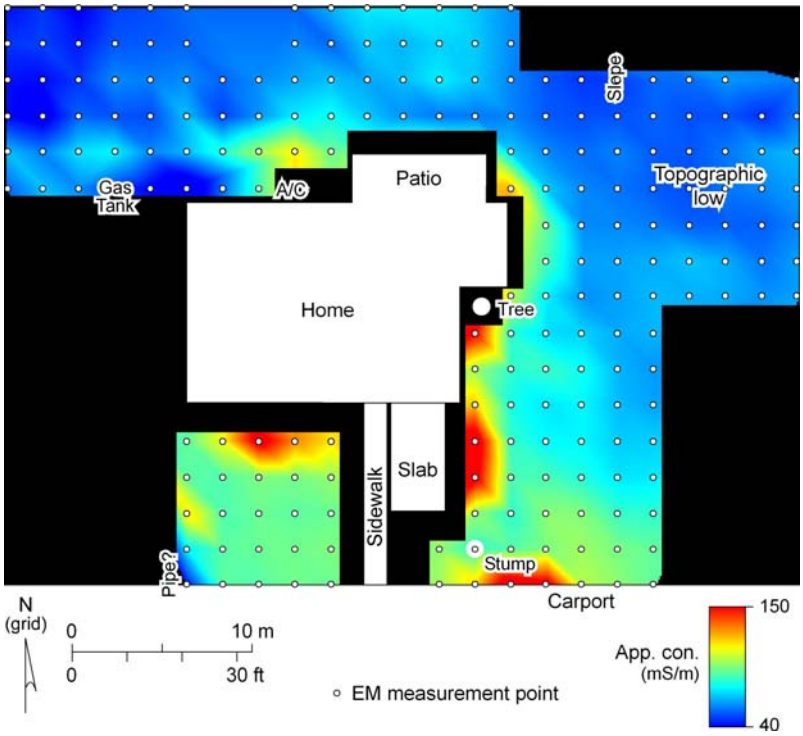

Figure 5. Apparent conductivity measured with a Geonics EM31 with the deeper-exploring vertical-dipole orientation and north-south direction.

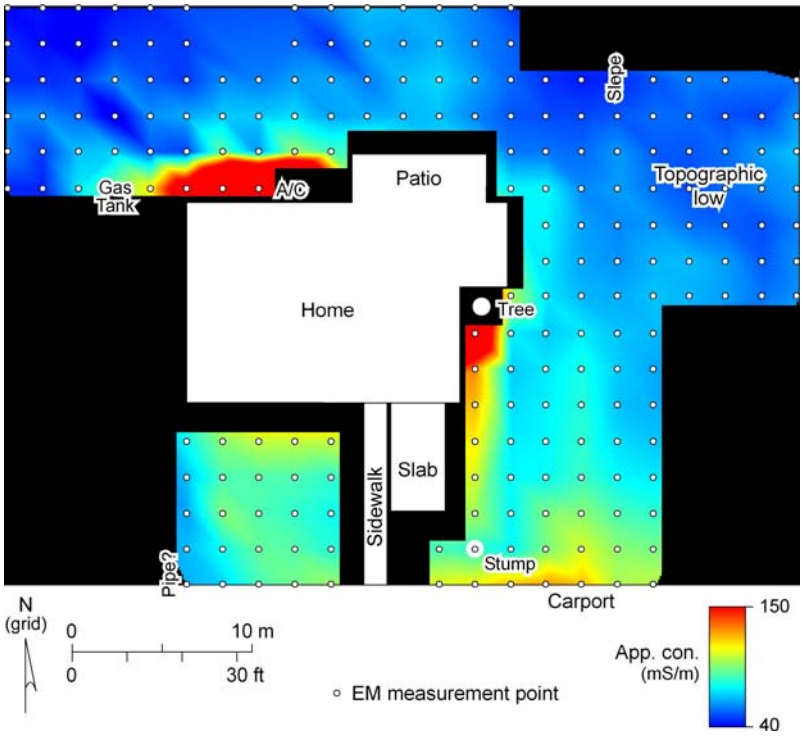

Figure 6. Apparent conductivity measured with a Geonics EM31 with the deeper-exploring vertical-dipole orientation and east-west direction.

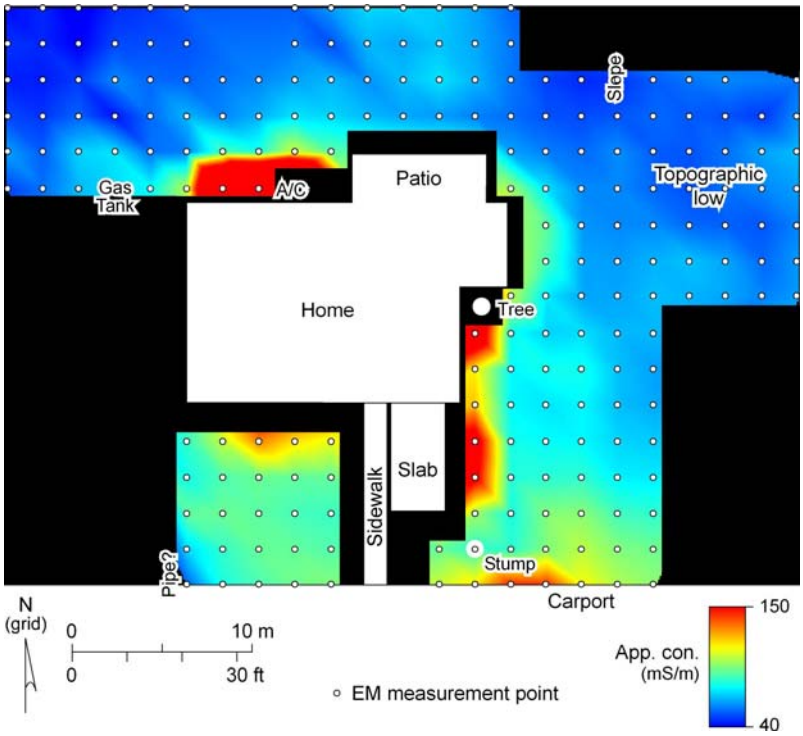

Figure 7. Average apparent conductivity measured with a Geonics EM31 with the deeper-exploring vertical-dipole orientation in the north-south and east-west directions.

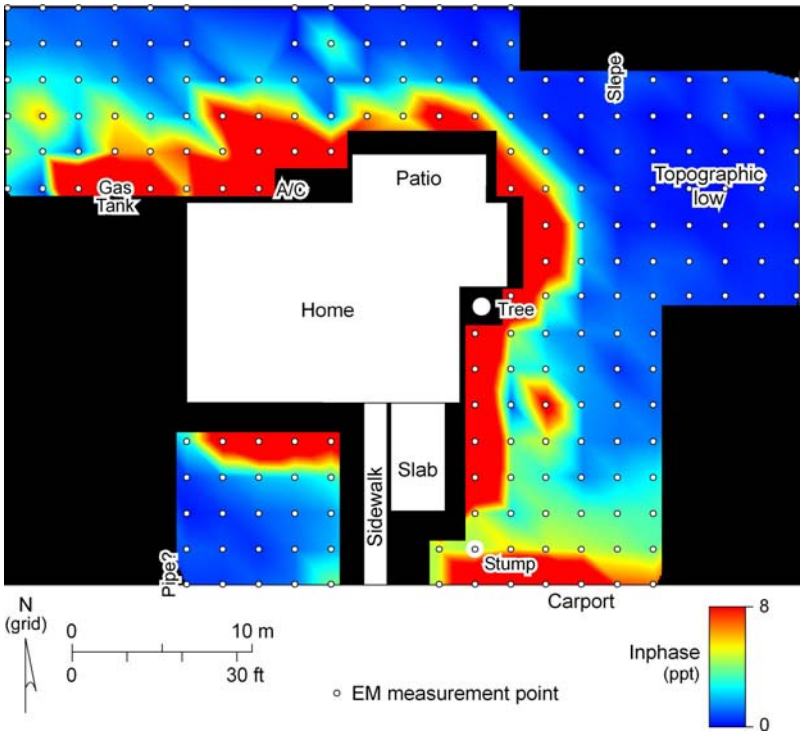

Figure 8. Average in-phase response measured with a Geonics EM31 with the deeper-exploring vertical-dipole orientation in the north-south and east-west directions.

Seismic Data

Seismic pulses generated from nine locations west of a small known void beneath a concrete slab passed beneath the slab, arriving at an array of 18 geophones located at fixed locations along a line east of the slab (table 1 and fig. 9). The source and receiver lines are parallel and are 8-m apart. Travel distances between the 180 pairs of paths from source to receiver ranged from 8 to 13.2 m. Elapsed time between the initiation of the seismic pulse and its arrival at the geophone ranged from 14.0 to 23.4 milliseconds (fig. 10); combining straight-line distances with elapsed times yields average propagation speeds of 373 to 602 m/s. Typical propagation speeds for compressional seismic waves in semi-consolidated clastic materials range from more than 300 to perhaps 800 m/s. The speed of sound in air, the material filling the shallow void, is about 340 m/s. The presence of a significant void along the path of a seismic wave can affect the propagation speed of the wave, typically resulting in a slowing of the wave, a delay in arrival time, and a lower average propagation speed on paths from source to receiver that intersect the void.

Velocities calculated from the first-arrival times at each of the 18 geophones for each of the seismic shot points show a consistent reduction in velocity between geophones 9 and 17 (fig. 11), suggesting that low-velocity material is present adjacent to these geophones. These geophones extend from row 12.75 to 14.75 (fig. 9), which roughly corresponds to the position of the void beneath the concrete slab.

The arrival times and calculated velocities can also be combined in an attempt to produce an image of the seismic velocity distribution between the source and receiver lines. There are several approaches of differing rigor to accomplishing “tomographic” imaging, but the approach we attempted in this preliminary test was to assume straight-line paths from sources to receivers (no wave refraction at velocity interfaces), assume the average velocities calculated for each source and receiver pair applied to every point along the path between that source and receiver, collate all positions and average velocities, and then grid all the measurements using a relatively coarse cell width (20 cm). Cell velocities binned and gridded from these data will not represent the true subsurface velocity distribution, but should reveal areas where there is a consistent slowing of seismic velocity. For example, average velocities calculated for all source-receiver paths along column 13.7 (fig. 12) show a decrease of about 100 m/s from north to south, indicating that low-velocity material exists for source and receiver paths crossing the southeastern part of the space between the source and receiver lines. Combining data from all source and receiver paths at 20-cm intervals across the space between the source and receiver lines yields a smoothed tomographic image of velocity variation between the lines (fig. 9). This image depicts a low-velocity area in the southeastern part of the image. The northwestward boundary of the low-velocity area coincides with the approximate location of a filled surface opening adjacent to the sidewalk and the current surface opening on the eastern edge of the concrete slab. The significant reduction in seismic velocity is most likely related to the known void beneath the slab, which would delay the arrival time for source-receiver paths that intersect the void. The southeastern boundary of the low-velocity zone cannot be determined from the available data because the number of source-receiver paths decreases as the edge of the image is approached.

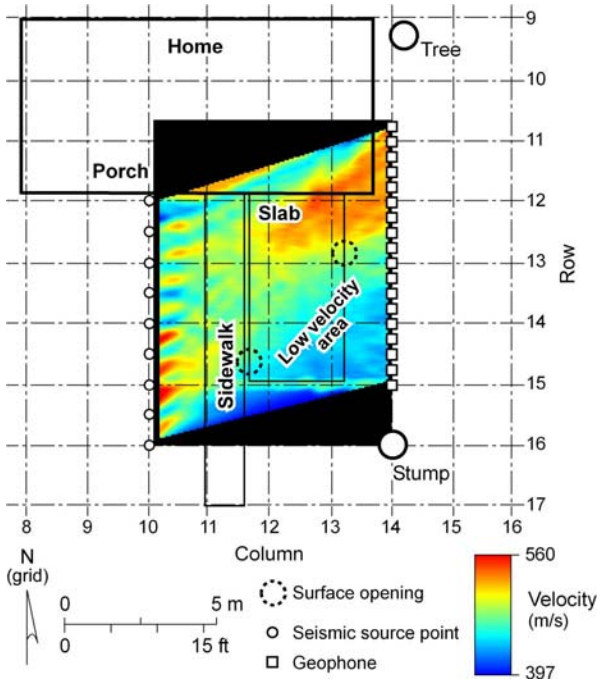

Figure 9. Seismic test at the Dempsey residence. Nine hammer source locations are separated by 1 m along grid column 10 west of the sidewalk; 18 receiver locations are separated by 0.5 m along grid column 14 east of the concrete slab covering the voids. The approximate location of current and former surface openings is outlined. A tomographic image depicting seismic velocity changes in the shallow subsurface between the source and receiver lines shows a low-velocity area in the southeast portion of the image.

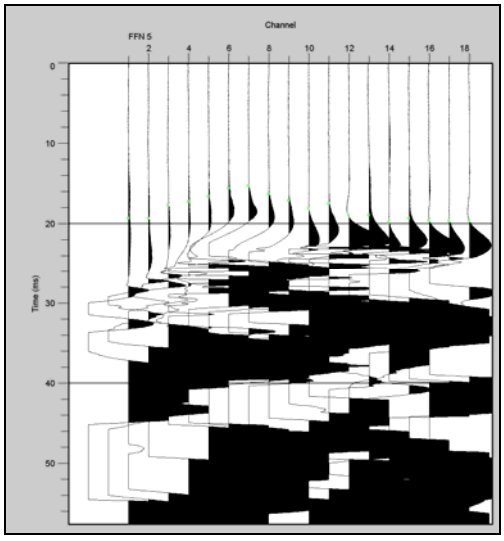

Figure 10. Ground motion recorded at geophones 1 (left) through 18 (right) for Timpson seismic file 5.dat (table 1). Only the first 58 milliseconds are shown. Small green dots indicate the interpreted first-arrival time. Variations in arrival time for differing source points and receiver pairs were used to interpret propagation velocity variations between the source and receiver lines.

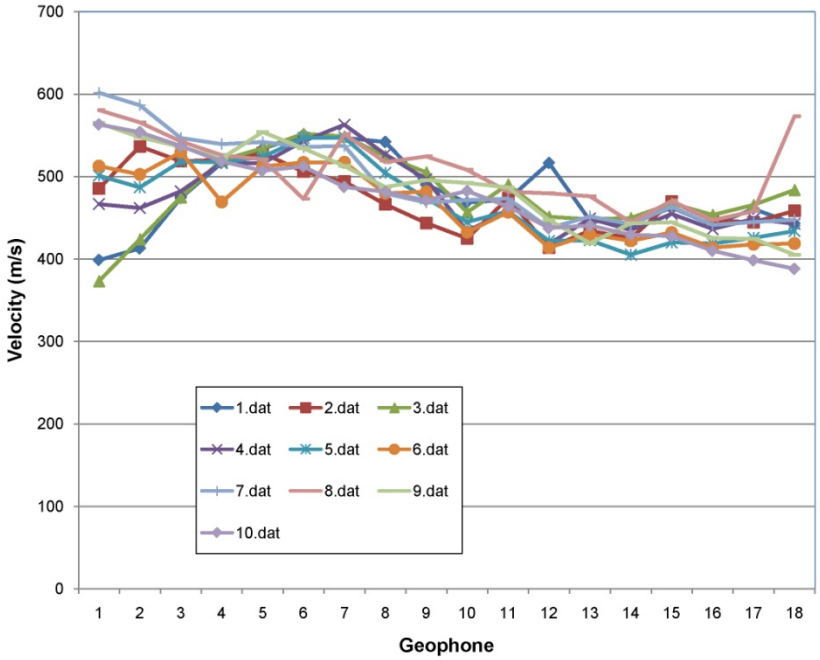

Figure 11. Average velocities calculated for arrivals from all seismic shots (table 1) at each of the 18 geophones. Relatively low velocities are calculated for geophones 9 through 17.

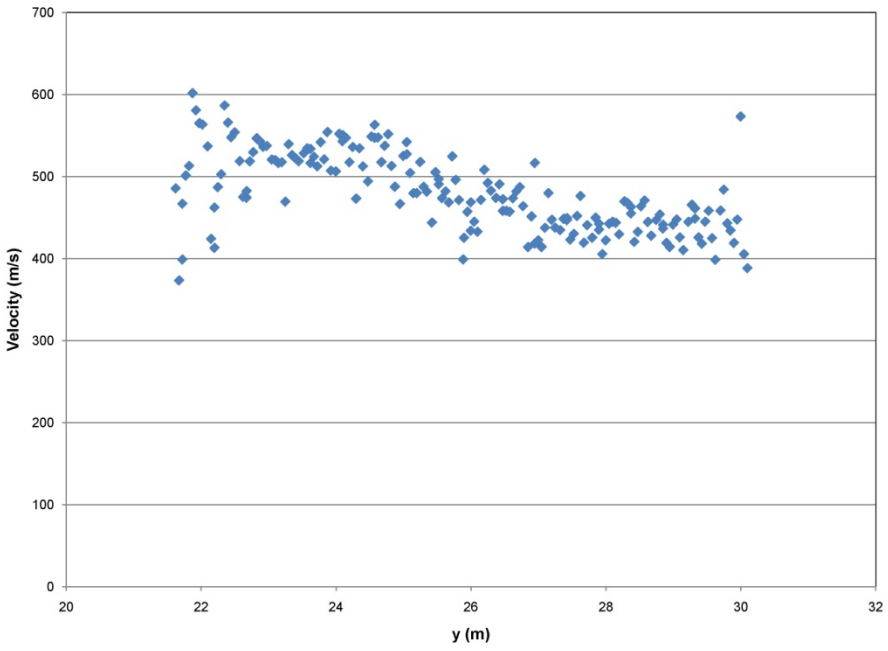

Figure 12. Average velocities calculated for arrivals from all seismic shots (table 1) as they pass through column 13.7. Decreased velocities are evident at y values between 25 and 30, which corresponds to rows 12.5 to 15.

Conclusions

Electromagnetic induction and preliminary seismic measurements acquired at the Dempsey residence were intended to identify whether significant voids are present at the site within the exploration depth range of the instruments used. The EM data, acquired using an instrument with a nominal maximum exploration depth of about 6 m, revealed no unequivocal voids within that depth range. Anomalous low conductivity areas east of the residence are associated with areas that have been previously backfilled. Some of these anomalies are near other EM anomalies that suggest the presence of significant amounts of buried metal that could have been part of the backfill. EM or resistivity equipment capable of reaching the anticipated depth of historical mine workings (15 to 20 m) are required to determine whether there is evidence for voids at depths greater than about 6 m. Frequency-domain EM instruments similar to the Geonics EM34-3 or time-domain instruments would be capable of reaching sufficient depth, but their practicality at this site will be limited by available working space and by cultural features that include the house, buried pipes and other large metallic objects, and power lines.

Seismic testing across a known void beneath a concrete slab yielded promising results. The void appears to locally increase arrival times and decrease average velocities for waves that intersect the void. A tomographic image produced for the area between the source and receiver lines shows a significant reduction in seismic velocity that coincides with the location of former and current surface openings associated with the void. A more comprehensive seismic tomographic survey might be useful at this and similar sites. One possible application would be to locate sources and receivers on opposite sides of an at-risk structure to identify low-velocity zones beneath the structure that would indicate the most likely locations of voids in preparation for verificatory drilling.

Acknowledgments

Research described in this report was sponsored by The Railroad Commission of Texas (RRC) under Contract No. UTAA8-066. Jon Brandt served as project manager at RRC.

References

Frischknecht, F. C., V. F. Labson, B. R. Spies, and W. L. Anderson, 1991, Profiling using small sources, in Nabighian, M. N., ed., Electromagnetic methods in applied

geophysics—applications, part A and part B: Society of Exploration Geophysicists, p. 105-270.

Geonics, Ltd., 1991, EM31 Operating Manual: Geonics Ltd., Mississauga, Ontario, 62 p.

McNeill, J. D., 1980a, Electromagnetic terrain conductivity measurement at low induction numbers: Geonics Ltd., Mississauga, Ont., Technical Note TN-6, 15 p.

McNeill, J. D., 1980b, Electrical conductivity of soils and rocks, Geonics Ltd.: Mississauga, Ont., Technical Note TN-5, 22 p.

Paine, J. G., and Collins, E. W., 2001, Urban geophysics at the Burger Activity Center in southwest Austin: noninvasively mapping covered strata at a possible sinkhole, *in* Woodruff, C. M., Jr., and Collins, E. W., field trip leaders, Austin, Texas, and beyond—geology and environment: a field excursion in memory of L. Edwin Garner: Austin Geological Society Guidebook 21, p. 79–87.

Paine, J. G., and Collins, E. W., 2003, Ground-based geophysical investigations in the Seco Creek area, Medina County, Texas: The University of Texas at Austin, Bureau of Economic Geology, final report prepared for U.S. Geological Survey, under Order No. 02CRSA0768, 36 p.